CHAPTER II

LITERATURE REVIEWS

This chapter describes the literature reviews of silica from rice husk ash, which include thermal decomposition of the rice husk, phase transformation of its ash at elevated temperatures and its resultant specific surface area. The raw materials, rice husk ash from power plants and waste sediment from aluminum industry, are stated. Mullite synthesis and processing, its properties and applications are mentioned. In addition, slip casting, its process and properties, are briefly explained.

2.1 Silica from Rice Husk Ash

Rice husk ash (RHA) comes from the combustion of rice husk (RH), and its disposal or utilization remains a major concern. RH generally consists of 38% cellulose, 22% lignin, 20% ash, 18% pentosans and 2% of other organic matters. The compositions depend on the variety, climate and geographic location [4]. The presence of silica in RHA has been known since 1938 [16]. Silica in amorphous form is present all over the husk structure but is concentrated on the outer and inner epidermis [3, 17]. High purity silica may be extracted from RH in the following steps. RH is thoroughly washed with water to remove adhering soil and dust and then leached by HCl, H_2SO_4, HF and HNO_3. These acid treatments are effective for the removal of impurities and also have effects on phase and specific surface area of silica. After acid treatment, the RH is pyrolyzed to burn out organic substances and high purity silica remains. Changes with temperature during the pyrolysis of RH will be explained in the following sections.

2.1.1 Thermal Decomposition of RH

Thermal decompositions of RH can be investigated by dynamic thermoanalytical techniques such as: Differential Thermal Analysis (DTA),

Thermogravitic Analysis (TGA) and Differential Thermalgravitic (DTG). The thermal behavior is explained on the basis of the decomposition of cellulose and lignin that are major contents of RH. Mass loss occurs in three definite stages (Figure 2.1): i) a removal of moisture during 100-215 °C (A-B), ii) a release of volatile matter from 215-350 °C (C-D) and iii) burning of combustible materials during 350-690 °C (D-E) [4]. Incineration of the organic components of RH causes a high percentage of fine pores in the ash skeleton. Figure 2.1 shows ~ 55% weight loss of RH, an endothermic peak at 105 °C on the DTA curve during the removal of moisture and an exothermic reaction which peaks at 335 °C due to the release of volatile matter.

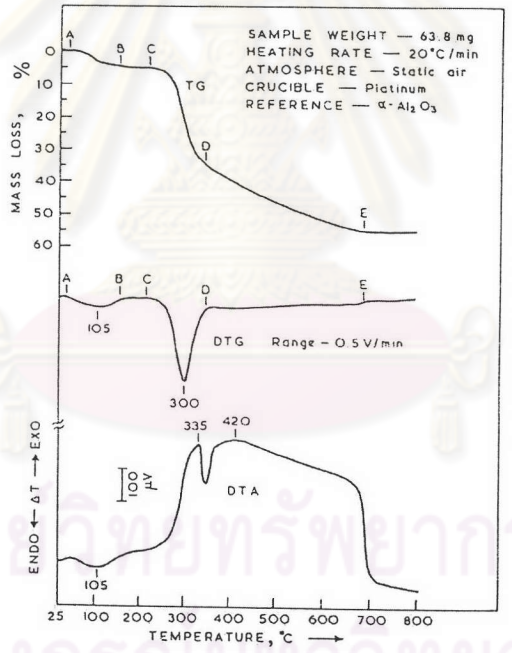

Figure 2.1 TGA, DTG and DTA curves of RH [4].

Concha Real et al [5] studied the pyrolysis of RH in air from 25-600 °C and in helium after 600 °C. After stabilized weight of RH at around 65% weight loss at ~ 600 °C, oxygen is replaced by helium while TGA in progress. A total weight loss of 79 % was observed indicating that RH contains 21% silica and 14% carbon.

At room temperature, silica phase in RHA is disordered. Differential Scanning Calorimetric (DSC) spectrum of RHA in Figure 2.2 [18] shows an exothermic peak at 135 °C indicating the transformation of low tridymite to high tridymite and four endothermic peaks at 190, 220, 235 and 250 °C representing the transformation of the cristobalite phase from low cristobalite to high cristobalite.

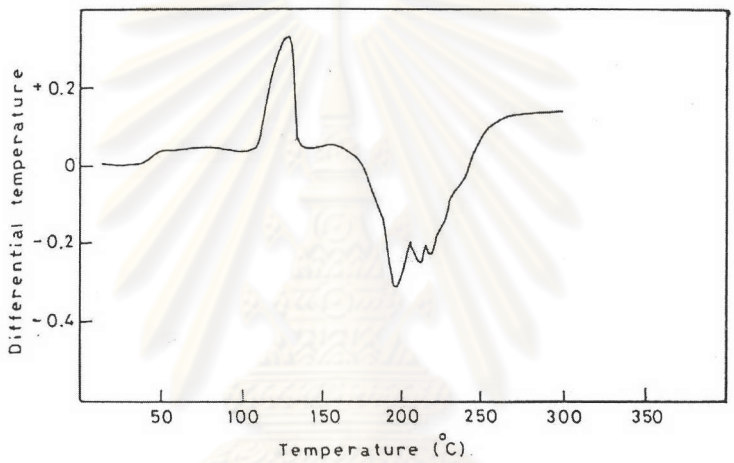

Figure 2.2 DSC of RHA fired at 1200 °C for 3 hours [18].

2.1.2 Transformation Phases of RHA at Elevated Temperatures

Polymorphic transformation of silica is summarized schematically below. The transformation can be either displacive or reconstructive. The displacive transformation is a slight rearrangement of the atoms in the structure without bond breaking. While the reconstructive transformation involves bond rupture and significant movements of atoms within the structure.

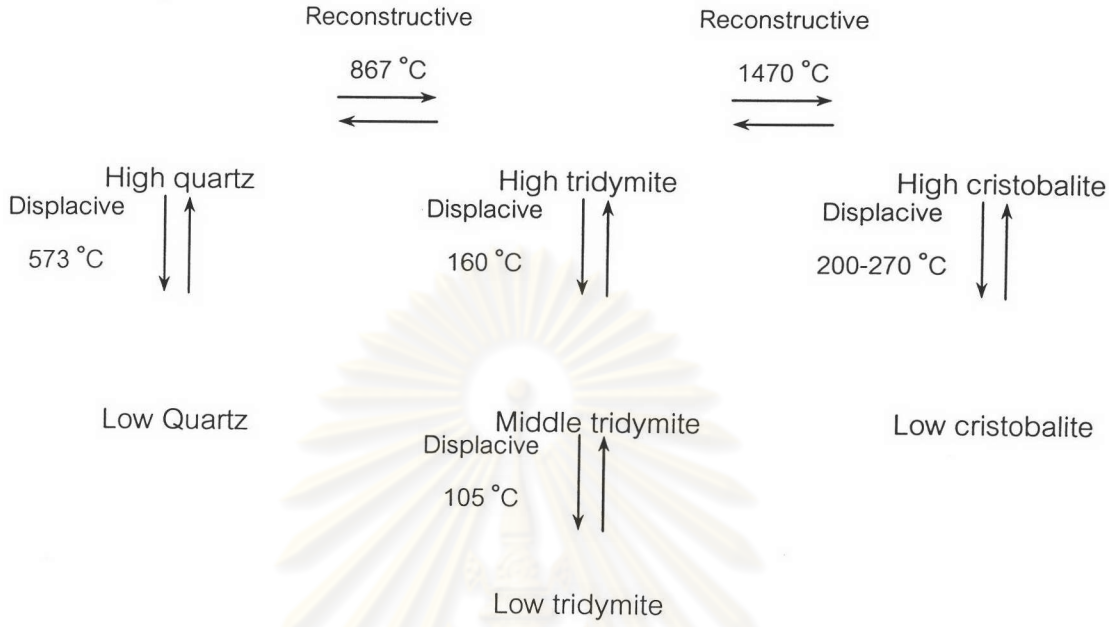

Curve (1) in Figure 2.3 represents X-Ray diffraction (XRD) patterns of RH and RHA from various temperatures. A hump at $2\theta = 22^{\circ}$ is observed in the samples fired below 600 °C, indicating the presence amorphous silica, which is attributable to the thermal insulation [19]. Crystallization of silica into cristobalite phase is noticable at 800 °C and more apparent at 900 °C [20, 21]. At higher temperature, tridymite phase forms inconjuction with cristobalite [20, 21].

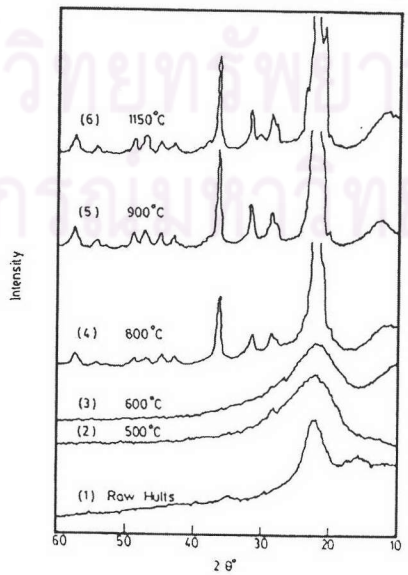

Figure 2.3 XRD pattern of RHA prepared at different temperature [21].

The changes of silica phase in RH with temperature can be written as

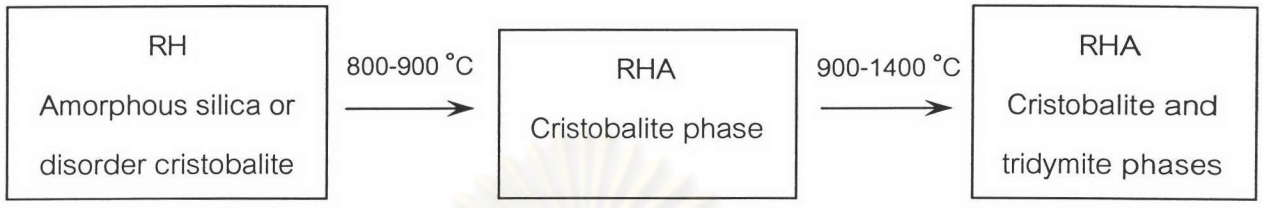

Potassium ion which is a major impurity in RH can stabilize tridymite structure [5]. Figure 2.4 shows the influence of K^+ cations in tridymite structure. XRD patterns of the heated husk (A) and aerosil silica with K^+ (A200K) illustrate the presence of tridymite phase. When K^+ is removed by acid leaching either before or after 1300 °C heat treatment, silica transforms to crystobalite instead (B and C). Metal addition, such as Fe, into aerosil silica does not cause a notable difference in transformation into cristobalite compare A200(1400 °C) with A200-Fe(1300 °C).

ศูนย์วิทยทรัพยากร
จุฬาลงกรณ์มหาวิทยาลัย

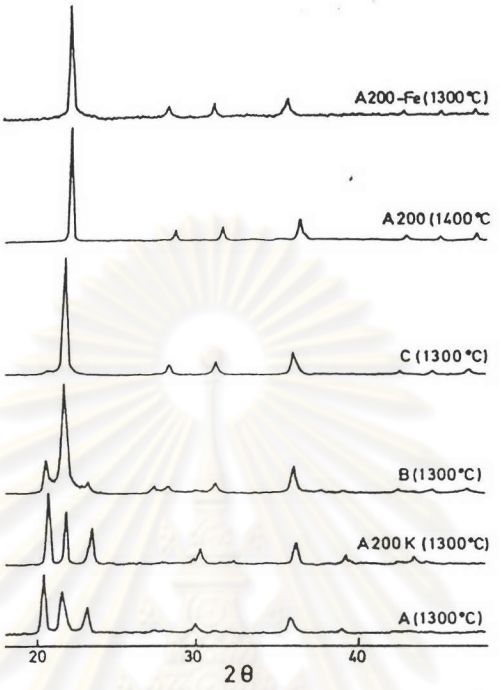

Figure 2.4 XRD patterns of RHA from different treatments [5],
(A is untreated rice husk , A200K is Aerosil silica added with K^+ cations,
B is RH treated with HCl after burning, C is RH treated with HCl before burning,
A200 and A200-Fe are aerosil silica and Fe added aerosil silica, respectively).

2.1.3 Specific Surface Area of RHA

Specific surface area (SSA) of RHA depends on both soaking temperature and time. From Figure 2.5, SSA peaks between 400-500 °C due to the development of pore structure in RHA. Increasing temperature and soaking time causes particle growth, a reduction of pore size and hence a decrease in SSA. A dramatic decrease of SSA between 800-900 °C is resulted from a sharp increase in crystallite size and probably also the conversion of silanol groups to siloxane bridges, which leads to pore opening corresponding to the appearance of cristobalite phase [4].

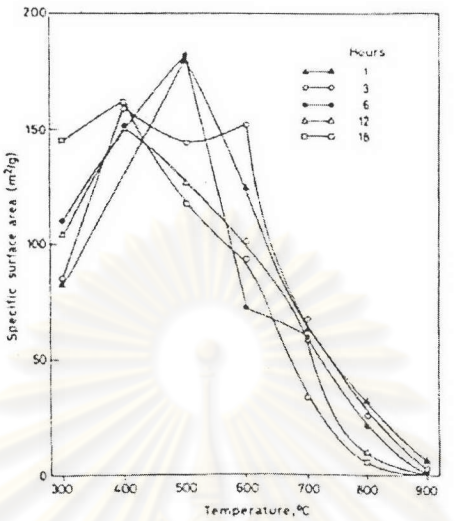

Figure 2.5 Variation of SSA of RHA with different temperature and soaking time [4].

A removal of alkali and alkaline earths impurities from RH affects the SSA [5]. SSA of RH with and without treatment is given in Table 2.1. The SSA of the untreated (A), and HCl leached after burning (B) are < 1 m^2/g. Pretreatment with HCl (C600 °C and C800 °C) or water before burning raises SSA. It is explained that low SSA of A and B are due to the interaction of some impurities with silica during the heat treatment of RH. The SSA of C and D is higher because the alkali and alkaline earths impurities were removed by acid leaching and water treatment, respectively.

Table 2.1 SSA (S_{BET}) and specific pore volume of calcined RH [5]

Sample*	S_{BET} (m^2/g)
A	< 1
B	< 1
C (600 °C)	260
C (800 °C)	211
D	209

A: untreated

B: carbon burnt out then HCl leached

C: HCl leached then burnt

D: water rinsed then burnt

2.2 Rice Husk Ash from Power Plants

Amount of RH fed to power plants in Thailand increases year by year because it is available in huge amount all over the country and cheapest when compared to other types of fuel. Nowadays, there are more than 20 small and large size power plants and more than 450,000 tons of RHA is estimated for each year.

RHA has been utilized domestically to some extent. For example, it is added in the materials for normal and lightweight brick making, to improve thermal insulation. Some is used to mix with soil for agricultural purposes.

Research and development on RHA applications has been carried out intensively in cementitious materials for concrete utilization [22], soil adjustment for agriculture [23] and also in lead filter for wastewater treatment in battery factory [24]. High silica content and abundant amount of RHA has attracted materialists to investigate possible application. However, the study in this field is not fully extended. The utilization in other fields is still not well-established and far to saturate.

2.3 Aluminum Hydroxide from Waste Sediment of Aluminum Industry

Waste sediment (WS) has aluminum hydroxide ($Al(OH)_3$) as the major component. Commercial grade $Al(OH)_3$ can be used for flame retardant, absorbent, emulsifier, antacid and filtering medium. WS is extracted from the drained water from the aluminum anodizing. This electrochemical process provides corrosion, wear resistance and decorative finishes by building up protective aluminum oxide layers. After this process, the treated surface is washed out, some oxide debris comes off with the drained water as the sediment.

In Thailand, the sediment was previously considered as waste. But recently it is used as a cheap filler in toothpaste and detergent. Also, it has been found that it can be synthesized to alumina powder [25].

2.4 Mullite

Mullite in natural materials is found embedded in a glassy phase matrix of mineral buchite. It is rare in nature but can be produced artificially. Mullite is an important phase in most conventional ceramics, e.g. clay products, pottery, porcelain and sanitaryware.

2.4.1 Composition Structure and Phase Relation of Mullite

Mullite is a constituent of ceramic products made from aluminosilicates. In fact, it is a non-stoichiometric solid solution having the structural formula $Al_2(Al_{2+2x}Si_{2-2x})O_{10-x}$, where x is a function of temperature and varies from 0.17 to 0.59. x=0 represents the polymorphic modification sillimanite, andalusite and kyanite (Al_2SiO_5), while x=1 represents the composition of Al_2O_3 [26].

Two mullites explained to be stable under atmospheric pressure are sintered and fused mullite. The former, formulated $3Al_2O_3.2SiO_2$, contains 71.8 wt% Al_2O_3 and 28.2 wt% SiO_2 and is called sintered mullite or 3/2 mullite (x=0.25) or stoichiometric mullite. It is produced by solid state reaction. The latter, $2Al_2O_3.SiO_2$, consists of 77.3 wt% Al_2O_3 and 22.7 wt% SiO_2 and is called fused mullite or 2/1 mullite (x=0.40). It is produced by melting the raw materials above 2000 °C and subsequent cooling to allow crystallization [27].

Two phase equilibrium diagrams of Al_2O_3-SiO_2 system has been proposed with the major disagreement whether mullite melts congruently or incongruently. From Figure 2.6, dash-dotted line, Bowen and Greig supposed one eutectic between silica and mullite about 1549 °C at E_1 and one peritectic reaction about 1828 °C at P_1 without solid solution [28].

However, Aramaki and Roy supposed two eutectic reactions, first between silica and mullite about 1597 °C at E_2 and second between mullite and

corundum 1843 °C at E_3. Mullite melted congruently and had a solid solution of 71.8-74.3 wt% Al_2O_3, and might reach 77.3 wt% Al_2O_3 under metastable condition [29].

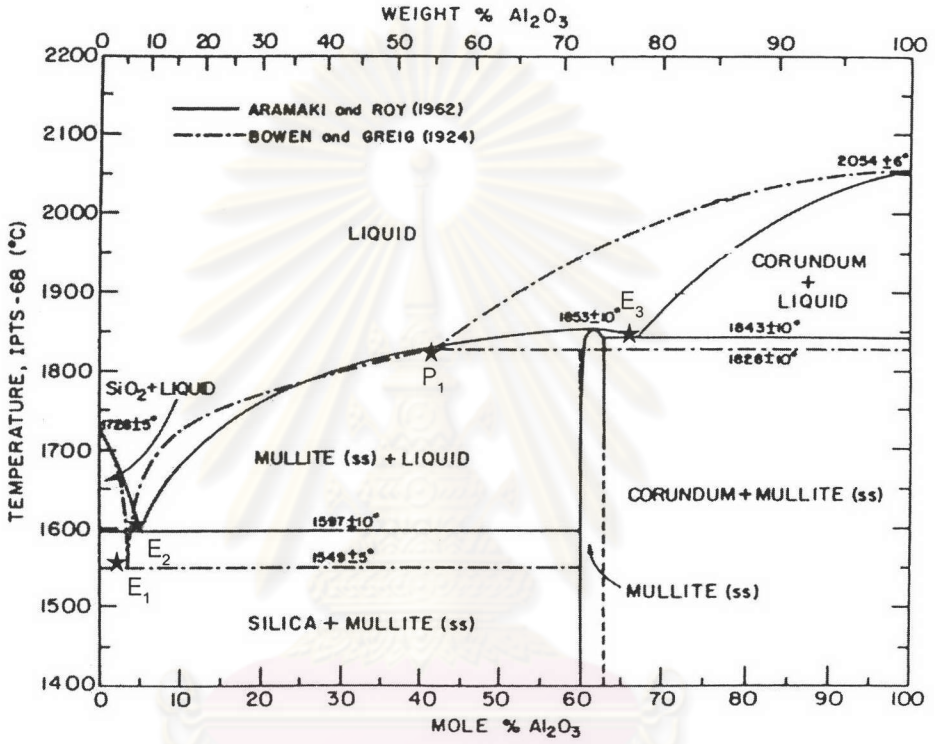

Figure 2.6 Phase equilibrium diagram of Al_2O_3-SiO_2 system [28, 29].

2.4.2 Mullite Synthesis

Mullite can be synthesized via various methods and may be classified in three types as following:

2.4.2.1 Sintered Mullite

Sintered mullite is prepared from mixed oxide, hydroxide, salts and silicates. Clay minerals such as kaolinite ($2SiO_2.Al_2O_3.\ 2H_2O$), pyrophyllite

($4SiO_2.Al_2O_3.H_2O$) and Al_2SiO_5 polymorphs (sillimanite kyanite and andalusite) are well known aluminosilicate minerals for mullite fabrication. Mullitization (mullite occurring) temperature is controlled by particle size of precursors because it takes place by solid-solid reactions or transient liquid phase reaction [30].

Kaonite transforms to mullite in the following steps (□ = vacancy) [31].

$$2Al_2(OH)_4[Si_2O_5] \xrightarrow{> 550\ ^\circ C} 2Al_2Si_2O_7 + 4\ H_2O$$

kaolinite — metakaolin

$$\geq 980\ ^\circ C: \quad 0.375Si_8[Al_{10.67}\square_{5.33}]O_{32} + SiO_2$$

$$\geq 980\ ^\circ C: \quad 0.188Al_8[Al_{13.33}\square_{2.66}]O_{32} + 4SiO_2$$

spinel phase — amorphous silica

$$\geq 1000\ ^\circ C: \quad 0.67(3Al_2O_3.2SiO_2) + 2.67SiO_2$$

3/2 mullite — amorphous silica

Al_2SiO_5 polymorphs tranforms to mullite according to the following reaction [29-31].

$$3Al_2SiO_5 \longrightarrow 3Al_2O_3.2SiO_2 + SiO_2$$

kyanite (1150 °C), or andalusite (1250 °C), or sillimanite (1300 °C) — 3/2 mullite — amorphous silica

Commercial sintered mullite for high temperature applications such as crucibles and tubes commonly uses kaolinite as a precursor. The quality of sintered mullite is limited by the impurity contents in the precursors.

2.4.2.2 Fused Mullite

It is fabricated by Czochralski method, which involves growing mullite single crystal of 2/1 composition ($2Al_2O_3.SiO_2$) [27]. For this method, mixture of Al_2O_3 and SiO_2 powders is heated to 1850 °C in nitrogen atmosphere and slowly cooled

down under controlled conditions such that desired Al_2O_3/mullite ratio and microstructure are obtained.

Raw materials for the production of commercial fused mullite are Bayer alumina, quartz sand, rock crystal and fused silica that are melted in an electric arc furnace at about 2000 °C.

2.4.2.3 Chemical Mullite

Chemical mullite is the mullite prepared by advanced processing processes such as sol-gel, precipitation, hydrolysis, spray pyrolysis, chemical vapor deposition (CVD). Mullitization routes are summarized in Figure 2.7.

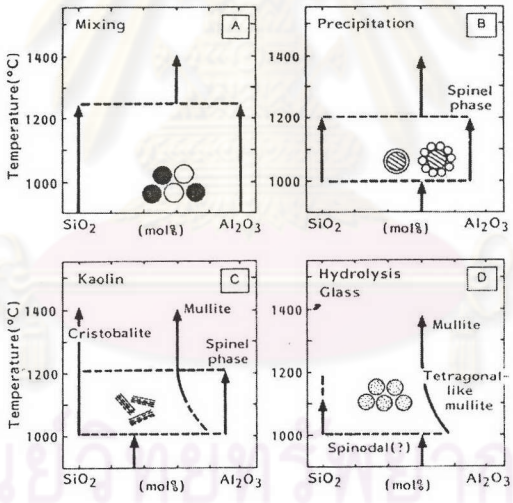

Route

Type A conventional mixing and sol-gel method

Type B precipitation method

Type C thermal decomposition of kaolin and Hydrolysis method without catalyst. Intermediate state between type B and D

Type D Hydrolysis method with catalyst

Figure 2.7 Mullitization routes [32].

2.4.3 Mullite Processing

2.4.3.1 Reaction Sintering of Al_2O_3 and SiO_2 Reactants

Starting materials for the reaction sintering of Al_2O_3 and SiO_2 reactants are admixture of clay and bauxite (refractory grade) and admixture of Al_2O_3 and SiO_2. Cost of mullitization process largely depends on the starting materials, their chemical purity, particle size and particle size distribution.

Sintering behaviors of quartz and α-Al_2O_3, cristobalite and α-Al_2O_3, silica glass and α- Al_2O_3 are shown in Figure 2.8.

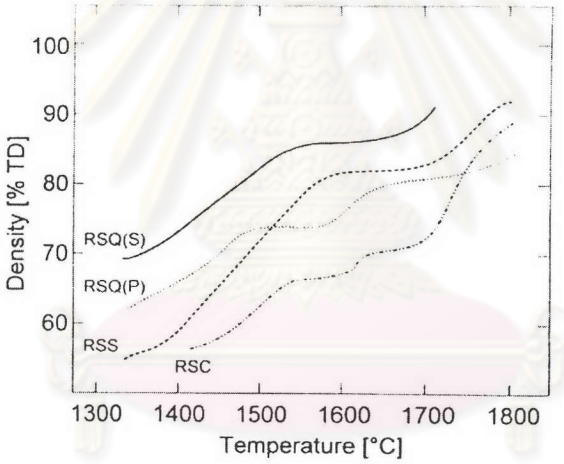

Figure 2.8 The sintering behaviors of RSQ (S): quartz and α- Al_2O_3 by slip casing, RSQ (P): quartz and α- Al_2O_3 by pressing, RSC = cristobalite and α- Al_2O_3, RSS: silica glass and α- Al_2O_3 %TD = % theoretical density [33].

RSQ (S) and RSQ (P) samples show extreme shrinkage between 1350 -1450 °C due to transient liquid phase from a small amount of the impurity in quartz. Densification occurs along liquid boundary layers around quartz. Shrinkage decreases to nearly zero above 1520 °C due to mullitization. The densification reincreases above 1650 °C by liquid phase sintering. Because of its preferable green

density, particle size and pore size distribution the slip casting samples show superior sintering densification to the other.

The shrinkage of RSC sample increases between 1450-1520 °C owing to solid state diffusion mechanism and is retarded above 1520 °C due to mullitization. Above 1600 °C, liquid phase sintering occurs by fusion of cristobalite resulting in higher shrinkage rate. At low temperature (≤ 1500 °C), the sintering densification of RSC is not prominent due to the absence of liquid phase.

The sintering densification rate of the RSS sample increases sharply between 1450-1550 °C with a decrease in viscosity of silica glass, and subsequently decreases due to the transformation of silica glass to cristobalite. Then after the transformation, the liquid phase sintering densification occurs in similar manner as in RSC sample.

2.4.3.2 Other Processing Routes

Sintering of mullite powder compacts requires temperature of >1700 °C because the diffusion of aluminum and silicon species takes place slowly. The densification is dependent on packing, surface area and size distribution of mullite powders [34].

Reaction bonding method of mullite comprising mullite plus Al_2O_3 can enhance mechanical strength [35]. Other processings are reaction sintering of chemical mullite and transient viscous sintering of composite powder.

2.4.4 Properties of Mullite

2.4.4.1 Mechanical Properties

Improvement of mechanical properties of mullite can be achieved by retaining smallest pore size, uniform grain size and minimal glassy phase at

grain boundary. Mullite derived from kaolinite and $Al(OH)_3$ has 95.6% relative density and a bending strength of 415 MPa at room temperature [36]. The strength can be improved by hot pressing technique. Figure 2.9 shows bending strength and fracture toughness of mullite in comparison with other materials.

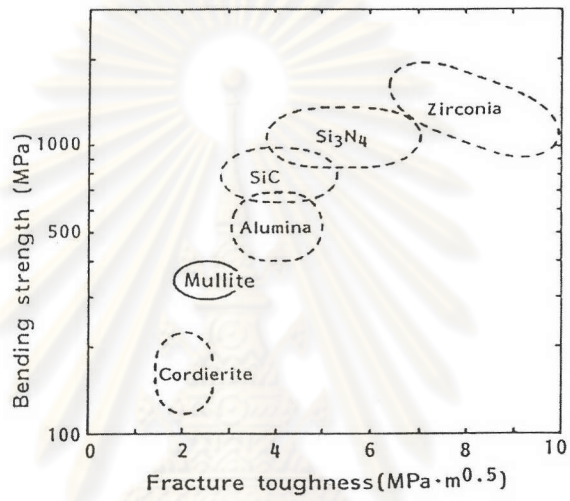

Figure 2.9 Bending strength and fracture toughness of mullite compared to other materials.

High temperature bending strength and fracture toughness of mullite as a function of wt% Al_2O_3 is depicted in Figures 2.10. A decrease in hot strength when wt% of Al_2O_3 > 66% does not relate to the presence of glassy phase at grain boundary but the enormous grain growth [37].

ศูนย์วิทยทรัพยากร
จุฬาลงกรณ์มหาวิทยาลัย

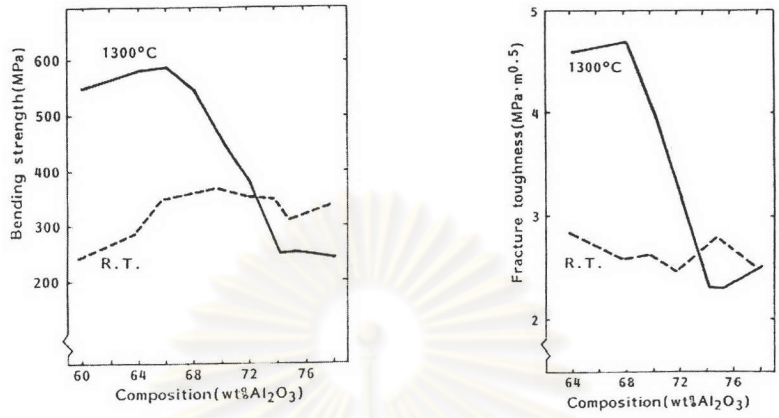

(a) (b)

Figure 2.10 (a) Flexural strength and (b) fracture toughness at room temperature and 1300 °C in air versus Al_2O_3 content.

Figure 2.11 shows that the microhardness of mullite declines slowly with increasing temperature, while that of Al_2O_3 and silicon carbide (SiC) decreases more rapidly. It is explained that at elevated temperature the mobility of dislocation is impeded by the complex domain structure of mullite, hence better microhardness than the other materials [38].

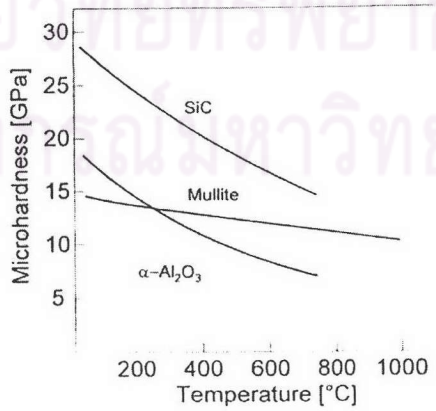

Figure 2.11 Microhardness of mullite, Al_2O_3, SiC as a function of temperature.

A lot of work has reported that creep resistance of mullite is influenced by the grain size. Poor creep resistance is found with large grain size samples [39]. Creep resistance of single crystal mullite at a stress level of 900 MPa at 1500 °C does not exhibit plastic deformation.

2.4.4.2 Thermal Properties

Thermal capacity of mullite rises sharply with temperature upto 800 °C and then slowly at higher temperature. The value typically ranges from 400 J $mol^{-2}K^{-1}$ at room temperature upto 550 J $mol^{-2}K^{-1}$ as shown in Figures 12 (a) [40]. Mullite has low thermal conductivity (5 W/mK at room temperature) when compared to other engineering ceramics. The thermal conductivity of mullite decreases with increasing temperature like other material as shown in Figures 12 (b) [41].

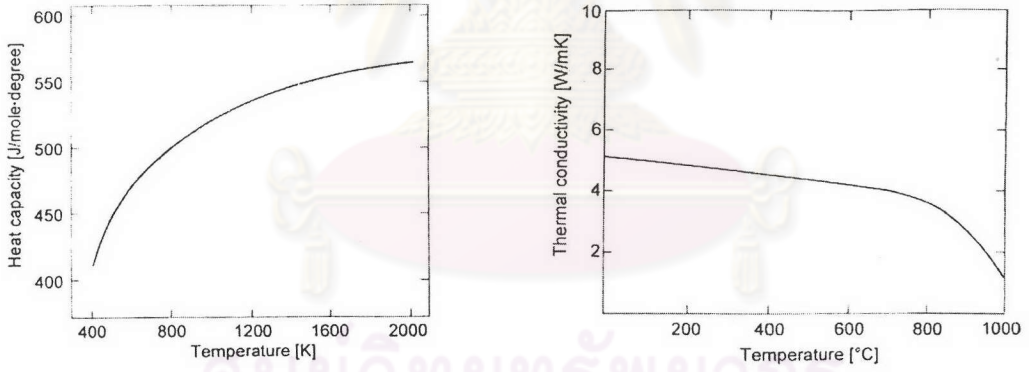

Figure 2.12 (a) Thermal capacity and (b) conductivity plotted versus temperature.

As a merit of its interlocking structure, mullite has thermal expansion coefficient as low as $5.1*10^{-6}$ °C^{-1} (25-1000 °C) and it is known to be a very good thermal shock resistant material [42].

2.4.4.3 Applications of Mullite

Mullite has some remarkable properties, e.g. high melting point (1890 °C), good creep and corrosion resistance and very good thermal shock resistance. Therefore, mullite and mullite composite ceramics is applicable to various applications.

It can be used as refractory in many industrial fields such as bricks and furnace linings for the steel-making and in melting chamber for glass industries, kiln furniture such as setting slabs, shelves and saggars, etc. Apart from these, mullite is widely used as a heat resisting material, for example, crucibles and protective tubes for thermocouples.

In engineering work, it is used as heat exchangers, honey combs, burner tubes, electronic packaging materials and laser activators.

2.5 Slip Casting

Slip casting is a well-known process for the production of conventional and some engineering ceramics such as pottery, porcelain products, sanitary ware, tube, engine components, etc. The process involves consolidation of solids from a stable suspension to form shapes. The suspension or slip may contain single or mixed ingredients [43].

This process is good for making some complex shapes, thin wall and closed-end products with extremely low production cost. The final product generally has good properties as a result of homogeneity of the mixture from wet milling and uniformity of the consolidation on casting.

However, this route has low production rate, low dimensional precision due to high shrinkage. Lifetime of plaster mold is shorten by slip corrosion. It is not suitable for large scale production, which a lot of molds and large working space are needed.

2.5.1 Slip Casting Process by Plaster Mold

Plaster or plaster of Paris is a mineral product made from calcined gypsum with half of water molecule ($CaSO_4.1/2H_2O$) remaining in the structure. A plaster mold is prepared by mixing the plaster with water, pouring into a case mold having the same shape as the required product, then allows to set. The plaster undergoes chemical hydration and turns to gypsum ($CaSO_4.2H_2O$). Needle-shaped crystals of gypsum form in random orientation interlocking throughout the body. Microvoids between the crystals provide a capillary suction pressure of about 0.1-0.2 MPa [44].

As a slip is filled in a plaster mold, the liquid is drawn capillarily from the slip into the plaster mold. The solid particles are forced towards the mold wall and a consolidated layer is gradually built up (Figures 2.13 (a)). For the drain casting, when a desirable layer thickness has been reached, the surplus slip is drained away (Figures 2.13 (b)). While for the solid casting (Figures 2.13 (c)), the process proceeds until a solid body is attained. Regularly, the cast body shrinks away from the mold before or during a subsequent drying process. Finally, the cast body is demolded and brought to fire.

ศูนย์วิทยทรัพยากร
จุฬาลงกรณ์มหาวิทยาลัย

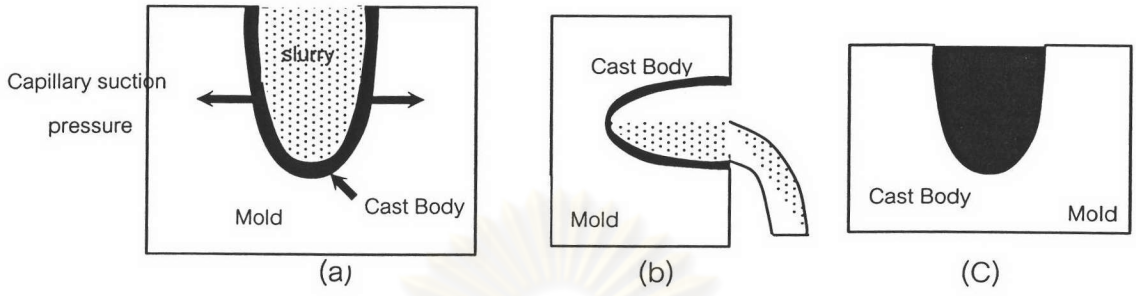

Figure 2.13 (a) The formation of cast body in slip casting.
(b) Drain Casting (c) Solid Casting

The diagram in Figure 2.14 summarizes a typical ceramic production process by slip casting. The slip is prepared by mixing and milling ceramic powders and additives such as deflocculants, deformers, binder and plasticizers in normal water or organic liquids. Proper proportions of the ingredients produce a slip suitable for the fabrication. Properties of slip may be explained in terms of rheology associated with surface chemistry.

ศูนย์วิทยทรัพยากร
จุฬาลงกรณ์มหาวิทยาลัย

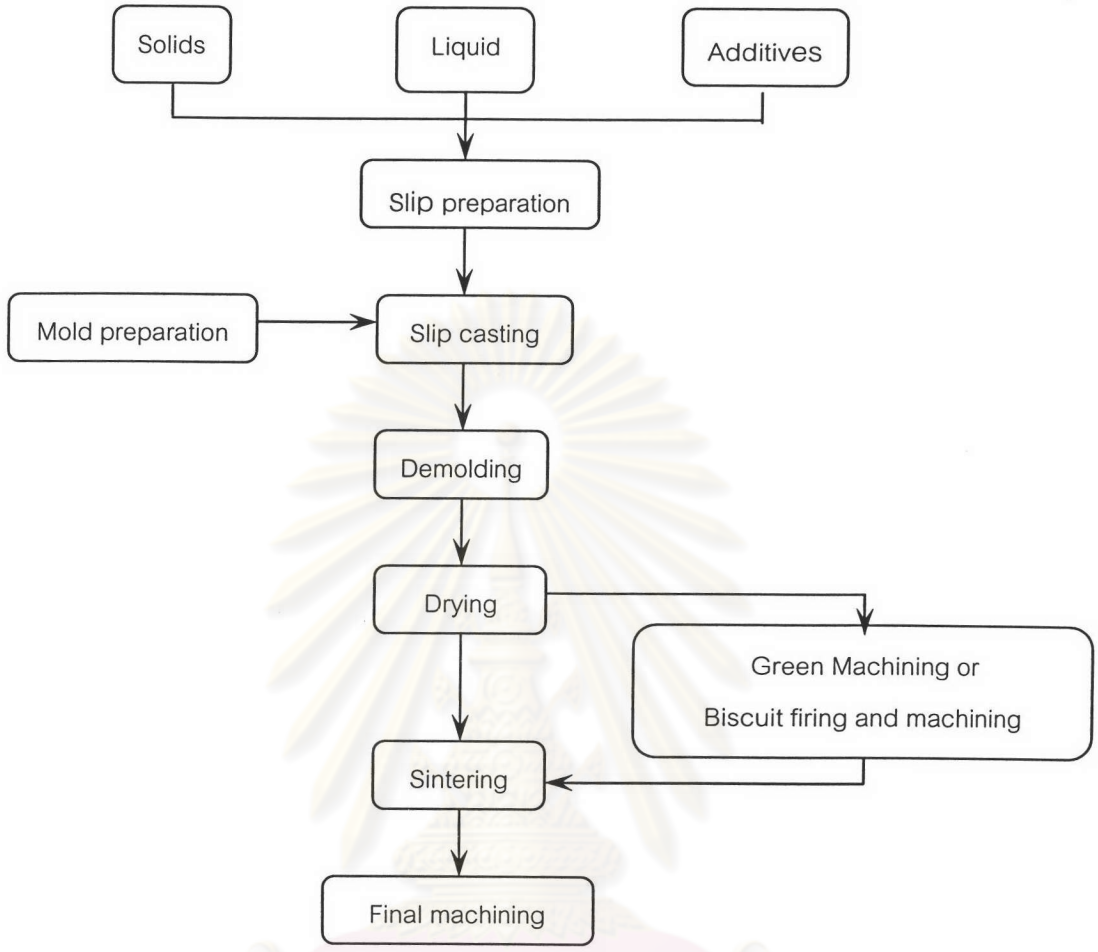

Figure 2.14 Diagram of a ceramic production process.

2.5.2 Surface Chemistry

Particle surface chemistry is a dominant factor affecting rheological properties of the slip as it regulates attractive and repulsive forces of the particles, which affect casting rate and microstructure of the final products. Control of surface chemistry can diminish defects introduced during casting, such as large isolated pores, segregation of particles and a spatial variation of packing density.

A basic concerned problem is the unstability of the suspension. The particle attraction is believed to be resulted from van der Waal attraction between particles and/or polarity of the medium. If the attractive force is large enough, the

particles will flocculate and thus rapid sedimentation. Some additives are therefore introduced to aid deflocculation.

Electrostatic stabilization is made use of the repulsion between electrostatic charges on the particle surfaces. Electrostatic charges can be chosen from deflocculants (dispersants) which are polyelectrolyte. They increase the repulsive forces by electrical charging interaction with a polar liquid medium. The deflocculants widely used for slip casting and tape casting are sodium carbonate, sodium silicate, sodium borate and tetrasodium pyrophosphate.

Polymeric stabilization arises from the repulsion between polymer molecules. This added organic (non-ionic) polymer molecules will adsorb or attach to surfaces of the particles.

The combination of the two stabilizations is electrosteric stabilization. To achieve this stabilization, the polyelectrolytes are used together with the polymers that have ionizable group such as sodium polymethacrylate, sodium polyacrylate and ammonium polyacrylate. The polyelectrolytes are used for advanced ceramics because of higher efficiency of stabilization and less residue in the fired body.

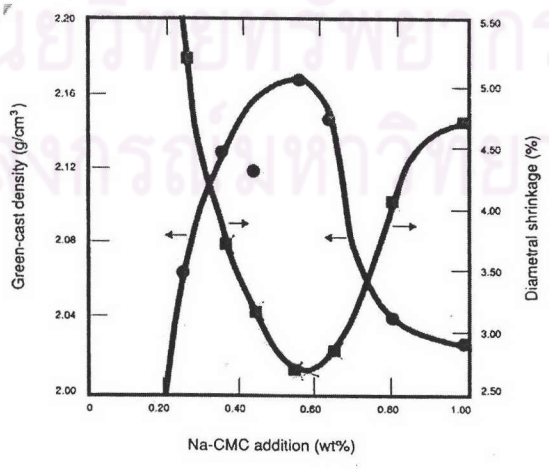

Figure 2.15 Green-cast density and % diametrial shrinkage of solid Al_2O_3 cylinders [45].

Figure 2.15 shows that the green-cast density and % diamentrial shrinkage of Al_2O_3 cylinders are optimized when 0.55 wt% Na-CMC (Sodium carboxymethylcellulose: polyelectrolyte) is added in the Al_2O_3 slip, i.e. the slip is best stabilized at 0.55 wt%.

A well-dispersed and stabilized slip will give a fairly dense and uniform cast. In practice, the casting rate of well-dispersed slip is low due to less permeability of the layer that has been consolidated to the mold wall. Therefore, the slip is practically made only partially deflocculated.

2.5.3 Rheology of Slip

Rheology is the study of viscous behaviors of fluids, suspensions and the being formed bodies that occur over the full range of applied shear condition. The characteristic property that describes the flow of fluid is viscosity (η), which is defined by

$$\eta = \tau / \gamma$$

where τ is the shear stress and γ is the shear rate. A common unit for viscosity is centiPoises (cP), which is equal to a milliPascal second (mPa.s).

Rheology properties of a given slip can be determined using the stabilization techniques. In general, a well-dispersed slip exhibits Newtonian flow (viscosity is independent of shear rate) at low particle concentrations. But when the particle concentration is relatively high and the viscosity depends on shear rate, the flow becomes non-newtonian.

There are two categories of rheology: time-independent and time-dependent rheology.

2.5.3.1 Time Independent Rheology

Figures 2.16 (a) and (b) shows six time independent rheologies. Changing shear rate causes a change in shear stress regardless with time. Newtoninan rheology such as water has a constant viscosity, and is independent of shear rate. It is opposite to Non-newtonian which the viscosity changes with the shear rate. If the viscosity decreases with increasing shear rate, it is called shear thinning or pseudoplastic rheology. Clay-water suspension shows this behavior. In contrast, if the viscosity increases with increasing shear rate, it is called shear thickening or dilatant rheology. Quartz-water suspension is an example exhibiting shear thickening rheology.

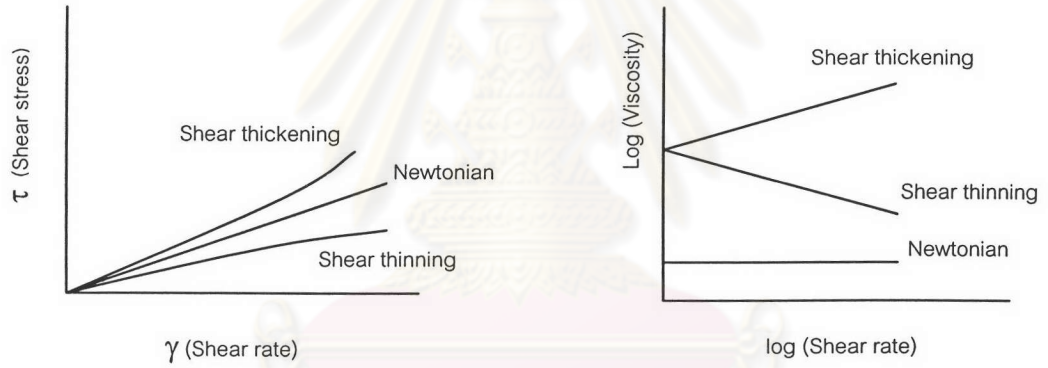

Figure 2.16 (a) and (b) Time-independent rheologies.

Figure 2.17 shows an effect of deflocculant on SiC slurry. T1128 (Targon 1128) is selected as it gives the lowest viscosity and stable slip. The SiC slurry exhibits shear thinning behavior.

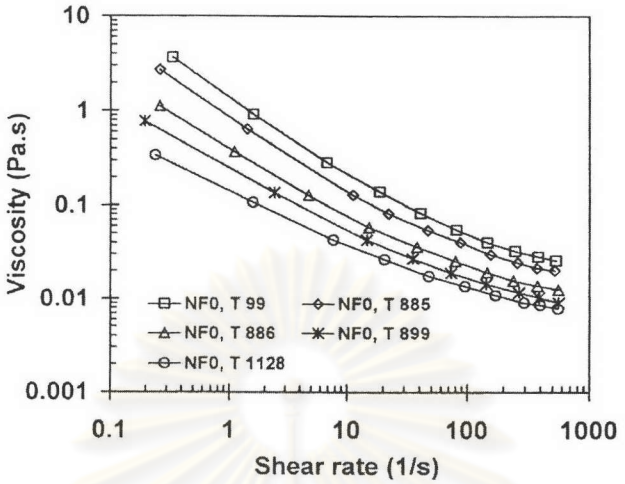

Figure 2.17 Steady-shear-viscosity curves of SiC (NFO: SiC commercial) slurry with 0.25 wt% of different deflocculants (T: Targon) [46].

2.5.3.2 Time-Dependent Rheology

Figure 2.18 shows two time-dependent rheologies, i.e. viscosity changes with time and shear rate: rheopexy and thixotropy. Rheopexy rheology shows an increase in viscosity with time at a constant shear rate. Rheopexy is time dependent shear thickening rheology. On the other hand, thixotropy shows a decrease in viscosity with time at a constant shear rate. Thixotropy is time dependent shear thinning rheology.

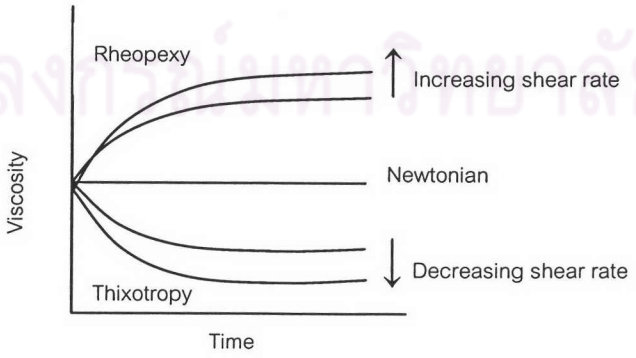

Figure 2.18 shows two time-dependent rheologies measured at constant shear rate

Casting slip are typical formulated to be shear thinning and have low viscosity. This behavior is convenient for mixing and pumping in mutual process. Properties of the slip adequate for casting include

- a deflocculated slip which gets low viscosity (high flow rate) to allow all parts of mold to be easily filled, to prevent trapping of air bubbles and easy drainage from the mold,
- high specific gravity to shorten casting time, increase green density, lower drying shrinkage and lower the amount of liquid medium.

ศูนย์วิทยทรัพยากร
จุฬาลงกรณ์มหาวิทยาลัย